

# **A Multi-Scale Predictive Model for Wafer Surface Evolution During a CMP Process Incorporating Slurry Evolution**

*Xiaoping Wang<sup>1</sup>, Pavan Karra<sup>1</sup>, Abhijit Chandra<sup>1,2</sup>, Ashraf Bastawros<sup>2,1</sup>, Rana Biswas<sup>3</sup>,  
Peter Sherman<sup>2</sup>, Lily Yao<sup>4</sup>*

*<sup>1</sup>Dept. of Mechanical Engineering, <sup>2</sup>Dept. of Aerospace Engineering, <sup>3</sup>Dept. of Physics  
and Microelectronics Research Center.*

*Iowa State University, Ames, IA 50011, USA*

*Email: [achandra@iastate.edu](mailto:achandra@iastate.edu)*

*<sup>4</sup>Strasbaugh Inc, San Luis Obispo, CA 93401, USA*

*Email: [lyao@strasbaugh.com](mailto:lyao@strasbaugh.com)*

## **Abstract:**

Predicting surface profile evolution is important in CMP because the success of control strategies to achieve global planarization depends on the accuracy and consistency of the underlying model. Wang et al (2005) have developed a model that predicts the evolution of surface profile based on pad-wafer interactions. The model however does not consider particle evolution over time. Han (2006) consider the agglomeration characteristics of slurry particles but apply them only at the particle scale. The current work incorporates particle agglomeration characteristics to predict the evolution of wafer at the die-scale. Both Reaction Limited Agglomeration (RLA) and Diffusion Limited Agglomeration (DLA) are considered, and their effects on die-scale profile evolution are investigated. Numerical simulations are performed and the results are compared with experimental data. A design map is provided as a guide for utilizing the model in practice.

## **1. Introduction**

Chemical Mechanical Planarization (CMP) is recognized as a promising planarization method in Integrated Circuit (IC) manufacturing. A detailed description of the CMP process can be found in several references (e.g., Steigerwald et al, 1997, Luo et al, 2004, Oliver, 2004). During CMP the wafer is held upside down by a rotating wafer carrier and is brought into contact with a polishing pad mounted on a rotating platen. Slurry containing abrasive particles is introduced at the interface between the wafer and the pad. A synergistic combination of the mechanical down force applied by wafer carrier as well as the chemical action of the slurry provides the polishing mechanism (Che et al, 2005). CMP is very effective in reducing the local step height. However, a global (die-scale) non-planarity may be generated (Figure 1) due to the differences in feature scale parameters (e.g., pattern density, line width) at different locations. This global non-planarity has a serious impact on subsequent process steps such as lithography and etching. The global thickness variation also impacts circuit performance: long-range clock wires passing through regions of different thicknesses result in different capacitances and may result in clock skew (Stine et al, 1997). Thus, development of an understanding of the effects of feature scale parameters on global planarization rates play an important role in optimization of the CMP process and layout density design.

Warnock (1991) has proposed a phenomenological model that allows quantitative prediction of wafer topography. In this model, the surrounding features affect the removal rate at a given point. Higher surrounding features decrease the removal rate, while the lower surrounding features enhance it. Three adjustable parameters have been used to describe the pad deformation, the pad roughness and the relative velocity respectively. The model predicted the experiment data very well. However these parameters have no direct physical meanings.

A contact wear model by Chekina et al. (1998) has been used to predict wafer topography evolution at the feature scale. The pressure distribution along wafer surface is studied based on contact mechanics, taking account of the elastic deformation of the polishing pad. Vlassak (2004) developed another contact mechanics based model, which takes into account both the roughness and elastic deformation of the polishing pad in computing the pressure distribution. Roughness of the pad is considered by the contact model of Greenwood and Williamson (1966). This model is able to evaluate the evolution of the wafer profile during the CMP process, but depends on an iterative solution procedure, where two equations describing the pressure distribution between the polishing pad and wafer, and the pad deformation needs to be iteratively solved. This procedure requires a significant amount of computation to reach convergence.

Ouma, et al. (2002) have developed a model to predict the wafer surface profile across a chip. A concept of “effective pattern density (EPD)” is introduced. The removal rate is assumed to depend on the effective pattern density and the blanket wafer polish rate (BWPR). The BWPR is determined by experiments. The estimation of EPD depends on pad deformation. In this model, it is assumed that the polishing of the down area does not start the up area is planarized completely.

Fu and Chandra (2003) have presented an analytical dishing and step height reduction model for CMP. They have assumed that i) the pad contacts with wafer at any point on the interface; ii) the higher area releases the pressure on the adjacent lower area; iii) the force redistribution due to pad bending is proportional to dishing/step height. This model gives analytical prediction for step height reduction and dishing. The bending factor  $\alpha$  that the authors introduced in their model to describe the force redistribution due to pad bending will be given a brief description later and used in this paper with some modifications.

In the present paper, a new multi-scale model is presented to describe the evolution of the wafer surface during a CMP process. The model considers the pad-particle wafer interactions via solid-solid contact. The time dependent particle evolution and agglomeration in the slurry is also incorporated in the model. The pad asperities are assumed with random height distribution, spherical tips, and periodical spacing across the pad surface. A solid-solid contact model based on the work of Greenwood and Williamson (1966) is utilized to determine the mean pressure at any point on the patterned wafer surface during a time step. In determining the mean pressure the visco-elastic pad relaxation is considered as in Guo et al (2004). A two term Prony series is considered to model visco-elastic pad. The parameters are fit to conform to the experimental data on pad relaxation reported by Borucki (2002). Once the mean pressure is determined, two approaches are proposed to re-distribute the pressure due to the effects of the surrounding topography at a given location. The modified pressure is then used to determine the local material removal rate (MRR) using particle scale indentation model for material removal (Wang C et al, 2005). The model is validated in section 3 against the experimental observations of Ouma et al (2002).

## **2. Model development**

For the sake of brevity, a summary of the multi-scale model development for wafer surface evolution during CMP is presented here. Figure 4 shows a flow chart of the simulation process. A solid-solid contact model is utilized at the particle scale, with the chemical reaction modifying the properties of the interface layers. This is augmented with a die scale model developed by Fu and Chandra (2003) and Kadavasal (2005). Following the approach of Warnock (1991) and Wang et al (2006), a non-local effect due to surrounding topography is introduced. Both time-independent elastic response, as well as the time dependent visco-elastic response of the CMP pad (e.g., Bastawros et al, 2002, Fu and Chandra, 2003) is considered. Finally, the slurry is

allowed to evolve or agglomerate. Reaction limited agglomeration (RLA) modes is considered for the evolution of particle distribution. (e.g., Han 2006).

### 2.1 Material removal rate (MRR)

Based on the above approach, the material removal rate (MRR) is given by

$$\overline{MRR}(x_i, t) = \frac{\Delta Z_w(x_i, \Delta t)}{\Delta t} = \frac{\Delta V_{(\Delta x)} \cdot n_{(\Delta x, \Delta t)}}{\Delta x \cdot 1 \cdot \Delta t} = \frac{6\chi v}{\pi} \cdot \left( \frac{P^*(x_i)}{2H_w} \right)^{\frac{3}{2}} A_f \cdot \underbrace{\frac{(D^2)_{avg} D_{max}}{(D^3)_{avg}} f(D_{avg})}_{\text{the effect of particle size distribution}} \quad (1)$$

The total thickness removed from the wafer surface at a point  $x_i$  during the time step  $\Delta t$  is computed by

$$\Delta Z_w(x_i) = MRR(x_i) \cdot \Delta t \quad (2)$$

By updating the wafer profile for every time step, a time history of the wafer profile is obtained.

### 2.2 Simulation process flow from die-scale to particle scale

In order to obtain the wafer profile evolution at the die scale, a three-scale modeling approach combining the effects due to die scale profile and those due to feature scale pattern structures are used. First, the die scale (global) profile is extracted to calculate the pressure distribution along the wafer while neglecting the detail pattern structure at the feature scale. The local pressure distribution is evaluated and is redistributed to account for pad bending effects. Also the pad profile evolution is considered to account for pad wear. Then, further pressure re-distribution is incorporated due to the finer feature scale structure and is corrected to satisfy moment balance (Wang et al 2006). The particle evolution by both DLA and RLA particle agglomeration are simulated to account for the changing particle volume distribution. The MRR is calculated based on particle scale indentation model. The wafer topography is updated to reflect the removed material and the process is continued. The simulation process is shown schematically in Figure 4.

## 3 Model Verification

In this stage, the model predictions of die scale global step formation due to variations in feature scale parameters (e.g., pattern density, line width, pitch) are validated against experimental observations of Ouma et al. (2002). The experiment is done on an Ebara polisher with IC1000 pads used over a sub-pad with a fixed thickness. The mask layout of one die used in the experiment is shown in (Ouma, 2002). It is 20mm×20mm and discretized into many blocks. Each block is 4mm×4mm with different pattern structures. The prefix D denotes pattern density. Each density structure consists of vertical lines and spaces of 100μm pitch (the length of the line width and the space width). For example, D10 means that the line width is 10μm and the space width is 90μm. The prefix P denotes pitch. The density for each pitch structure is fixed at 50% (equal line width and space width). For example, P20 means both the line width and the space width are 10μm each. Along the line L3 and L4, the pattern density gradually increases from block to block. The step pattern density is defined along the line L5. L6 has a constant pattern density but the pitch length for each block is different. The pre-CMP wafer has a patterned surface with the initial step height (the height difference between up area and down area) 0.6μm. In their experiment, the thickness is measured on the up area (line) and down area (space) at several locations.

### 3.1 Parameter Estimation

In the simulation, the nominal pressure is set as 34kPa under the assumption that the nominal pressure applied to each die across the wafer is constant. The properties of pad asperities given in (Stein, 1996) are used in the simulation. The parameter values for pad asperity properties are

presented in Table I. The distribution of pad asperity heights is characterized by Pearson IV distribution. The procedure used to estimate the pad asperity heights PDF can be found in (Wang C, et al 2005) and (Johnson, 1970). The Young's modulus  $E_p$  for IC1000 pad is assumed to be 29 MPa (Baker, 1996). Other parameters including  $l$  (the influence length),  $\alpha$  (the pad bending factor), and critical contact height (H) needed in the simulation are estimated as following:

*Influence length at feature scale ( $l_f$ ) and at die scale ( $l_d$ )*

The influence length is defined as a distance over which the pad bends. At the feature scale, the pad bending is influenced by the local pattern structure. On the mask layout shown in (2002), the pattern structure is periodical in each block. Therefore, the feature scale influence length  $l_f$  may be assumed to be the pitch length. In Part B of the simulation where the feature scale is considered, the influence length  $l_f$  is set to be the pitch length. As the polishing time increases, the variation of die scale (global) profile will be generated since the MRR is different in different regions of the wafer due to variations in pattern structures. Then the pad also bends to conform to the die scale (global) profile. The influence length at the die scale can be characterized by the deformation length within which the pad surface will deform to follow the deformation of a loaded point. In other words, the MRR at a given point is influenced by its surrounding topography within this deformation length. The deformation length is defined as the planarization length in (Ouma, 1998). The approach to obtain this length has also been investigated there. Therefore the pad influence length ( $l_d$ ) in Part A of the simulation is approximated as 3mm, the average planarization length calculated from Table I in Ouma (2002).

*The pad bending factor  $\alpha$*

When the pad contacts with a patterned wafer, the contact pressure at a given point not only depends on the pad deformation at that point, but also depends on the pad deformation at the neighboring points. The zone of influence, over which the neighboring points affect a given point, has already been addressed by the influence length. But the extent or magnitude of the influence of the neighboring points for a given location is governed by the pad bending factor. The estimation of the pad bending factor can be obtained by the following:

The feature scale model prediction (step height reduction) is fitted to a single experimental data point to estimate the value for the pad bending factor. In the simulation for the experimental data in (Ouma, 2002) the step height reduction vs. time for the center point in each block on L5 may be used to estimate the pad bending factor since the global pad bending has a smallest effect there. From the experimental data for L5, we choose the data point at the location of 10 mm. The step height at 29 second for this location is about 0.33  $\mu\text{m}$ , it reduces to about 0.021  $\mu\text{m}$ . The pattern density is 0.3 and the pitch length is 100  $\mu\text{m}$  at this location. Using the feature scale simulation to evaluate the step height reduction at the selected point, the pad bending factor is found to be  $0.55 \times 10^{12} \text{ N/m}^3$ .

*The critical contact height H*

The critical contact height H is used to decide whether the low area of the wafer starts to be polished. It is different for different pattern structures and different applied pressures for a specified pad. In Cu CMP, dishing occurs due to the local pad bending. The saturation dishing depth (the asymptotic value of dishing for long time) for a non-selective slurry and elastic pad property is assumed to reflect the maximum pad bending depth, hence it may be assumed to be the critical contact height H. The values for each pattern structure are obtained from Laursen et al (2002).

### **3.2 Comparison of Simulation Results to Experimental Data**

The values for parameters used in the simulation are summarized in Table II. The Prony series parameters are given by [11]  $g_1^p = 26.67\%$ ,  $g_2^p = 20.72\%$ ,  $\tau_1 = 10\text{s}$  and  $\tau_2 = 300\text{s}$ . Figure 5 shows the model predictions (denoted by line) compared to the experimental data (denoted by points). The solid line and the solid points are the data for 29 seconds of polishing. The dashed line and the open points are for 88 seconds of polishing. The prediction error is also given with the root

mean square (RMS) in Table III.

From Figure 5 and the prediction error shown in Table III, it is observed that the simulation reliably captures the effects of the pattern density on the post-CMP wafer surface. At the region with lower pattern density, the up area thickness reduced faster. At the region with higher pattern density, the up area thickness reduced slower. Simulation is run without particle agglomeration first and then RLA and DLA agglomeration models are used separately to predict the wafer surface profile after 29 and 88 seconds. From the error table III it can be seen that while DLA does worse than the model without agglomeration, RLA does better than the other two. This is reasonable since it is quite likely that the slurry used in the experiments of Ouma et al (2002) has been stabilized. Moreover, results are presented for only 88 seconds of polishing. It appears that over this time period, the slurry agglomeration proceeds in the RLA mode rather than the faster DLA mode.

### **3.3 Prediction of scratch generation probability:**

Since the material removal essentially takes place by a scratching mechanism (e.g., Che, 2005), mean height reduction is governed by the mean indentation depth. In other words, if all particles indent to the same depth, then uniform material removal is achieved. It is the spatial variation in indentation depths that give rise to the phenomenon commonly referred to as “scratching”. To quantitatively identify or define a scratch, we must also define its severity. This is defined here as the ratio of a specific indentation depth compared to the mean value. Finally, maximum scratch severity in a particular process may be obtained by considering the ratio of the maximum indentation depth (defined either per unit area or over the entire wafer) to its mean value. The probability of such scratching events increases when particles agglomerate and increase in size, thus introducing few large particles in an otherwise good slurry. It has been found (Han, 2006) that due to DLA agglomeration process, the average particle size increases at a relatively fast rate. Reaction Limited Agglomeration (RLA), which is expected to be present in the experiments of Ouma et al (2002), and is typically much slower, is considered for the current work.

Apart from this agglomeration, pad relaxation due to viscoelastic response also takes place in a CMP process. Such viscoelasticity can significantly reduce the scratch generation probability, particularly over longer time periods needed to polish multiple wafers. The scratch generation probability, for the example considered in this paper, is shown in Table IV. Work is underway to also account for the increase in local stiffness of pad asperities due to pad wear effects (Bastawros et al 2002).

## **4. Conclusion**

A multi-scale model is proposed to evaluate the wafer surface evolution during a CMP process. The interface pressure between a patterned wafer and a rough pad is evaluated based on the work of Greenwood and Williamson (1966). Two pressure re-distribution methods are proposed to take into account the non-local effects of surrounding topography as well as cell level bending of the pad. The model predictions are first verified against experimental data of Ouma et al. (2002). The parameter estimation procedure used in the model is discussed. It appears that a better correlation between model predictions and experimental data is obtained when visco-elastic pad relaxation, as well as particle agglomeration in RLA mode is considered.

Clearly, the value of a mechanistic model lies in its predictive capability. Based on the limited comparisons against experimental data, it appears that the proposed model reasonably captures both spatial and temporal variations of the MRR. The following design map may be used to utilize such a model to predict the probability of scratching for a real-life CMP process:

- i) Estimate (off-line) pad material response for both elastic and viscoelastic

- deformation modes.
- ii) Evaluate in-coming Pad topography, and estimate relevant parameters.
  - iii) Estimate wafer material characteristics, and based on slurry chemistry, estimate the mechanical properties of the interface layer on the wafer surface.
  - iv) Evaluate in-coming wafer surface topography.
  - v) Specify process specifications (e.g., pressure, velocity etc.).
  - vi) Polish blanket wafer with intended slurry and pad. Estimate Preston Coefficient for pad wear.
  - vii) Polish patterned wafer (e.g., MIT mask). Utilize spatial distribution in MRR to estimate planarization length and pad bending parameter. Also utilize the temporal distribution (comparison of step height reduction for a time interval) to estimate the slurry agglomeration parameter.
  - viii) Predict Scratch Generation Probability with the Multi-Scale CMP model.
  - ix) Verify model predictions against experimental data.

Work is currently in progress to extend such a model and utilize it to predict scratch generation probability in a CMP process.

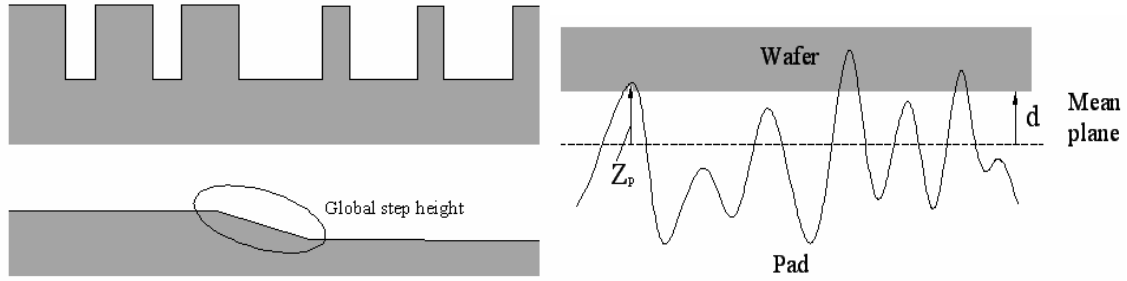
## 5. Acknowledgements

This material is based upon work supported by the U.S. National Science Foundation Grant Nos. CMMI-0323069 and CMMI-0640826. The authors gratefully acknowledge this support. Any opinions, findings and conclusions or recommendations expressed in this material are those of the authors and do not necessarily reflect views of the sponsoring agencies.

## References:

- Steigerwald, J.M., Murarka, S.P., Gutmann, R.J., 1997, Chemical mechanical planarization of microelectronic materials, John Wiley & Sons Pub., New York.
- Luo, J., Dornfeld, D. A., 2004, Integrated modeling of chemical mechanical planarization for sub-micron IC fabrication, Springer, Berlin Heidelberg, Germany.
- Oliver, M. R. (Ed.), 2004, Chemical mechanical planarization of semiconductor materials, Springer, Berlin, New York.
- Wei Che, Yongjin Guo, Abhijit Chandra, Ashraf Bastawros, A scratch intersection model of material removal during chemical mechanical planarization, *Journal of Manufacturing Science and Engineering-Transactions of the ASME* 127 (3): 545-554, Aug 2005.
- Stine, B., Mehrotra, V., Boning, D., Chung, J., Ciplickas, D., 1997, A simulation methodology for assessing the impact of spatial/pattern dependent interconnect parameter variation on circuit performance, *IEDM Tech, Digest*, pp. 133-136.
- Warnock, J., 1991, A two-dimensional process model for chemical mechanical polish planarization, *Journal of the Electrochemical Society*, Vol. 138, no. 8, pp. 2398-2402.
- Muthukkumar Kadavasal, Sutee Eamkajornsiri, Abhijit Chandra, Ashraf Bastawros  
Yield Improvement via Minimization of Step Height Non-Uniformity in Chemical Mechanical Planarization (CMP), 2005, MRS Spring Meeting.
- Bastawros, A.-F, Chandra, A., Guo, Y., Yan, B., (2002), "Pad effects on material-removal rate in chemical-mechanical planarization," *Journal of Electronic Materials*, Vol. 31, no. 10, pp. 1022-1031.
- Wang Xiaoping, Chandra, A, 2006, A Multi-Scale Model for Wafer Surface Evolution in Chemical Mechanical Planarization (CMP), *IEEE Transactions on Semiconductor Manufacturing*, Submitted.
- Chekina, O. G., Meer, L. M., Liang, H., 1998, Wear-contact problems and modeling of chemical mechanical polishing, *Journal of the Electrochemical Society*, Vol. 145, no. 6, pp. 2100-2106.

- Vlassak, J.J., 2004, A model for chemical–mechanical polishing of a material surface based on contact mechanics, *Journal of the Mechanics and Physics of Solids*, Vol. 52, pp. 847-873.
- Greenwood, J.A., Williamson, J.B.P., 1966, Contact of nominally flat surfaces, *Proceedings of the Royal Society of London*, A295, pp. 300-319.
- Ouma, O., Boning, D. S., Easter, W. G., Saxena, V., 2002, Characterization and modeling of oxide chemical–mechanical polishing using planarization length and pattern density concepts, *IEEE Transactions on Semiconductor Manufacturing*, Vol. 15, no. 2, pp. 232-244.
- Fu, G., Chandra, A., 2003, An analytical dishing and step height reduction model for chemical mechanical planarization, *IEEE Transactions on Semiconductor Manufacturing*, Vol.16, no. 3, pp. 477-485.
- Guo, Y., Chandra, A., Bastawros, A. -F., 2004, Analytical Dishing and Step Height Reduction Model for Chemical Mechanical Planarization (CMP) with a Viscoelastic Pad, *Journal of Electrochemical Society*, Vol. 151, no. 9, pp. G583-G589.
- Borucki, L., 2002, Mathematical modeling of polish-rate decay in chemical-mechanical polishing, *Journal of Engineering Mathematics*, Vol. 43, pp. 105-114.
- Wang, C., Sherman, P.J., Chandra, A., Dornfeld, D., 2005, Pad surface roughness and slurry particle size distribution effects on material removal rate in chemical mechanical planarization *CIRP Annals - Manufacturing Technology*, Vol. 54, no.1, pp. 309-312.
- Johnson, K. L., 1985, *Contact mechanics*, CUP, Cambridge, New York.
- Ying Ying Han, 2006, Scratch generation probability in chemical mechanical polishing process, Masters Thesis, Iowa State University.
- Preston, F.W., 1927, The theory and design of plate glass polishing machines, *Journal of Society Glass Technology*, Vol. 11, pp. 214-256.
- Archard, J. F., 1953, Contact and rubbing of flat surfaces, *Journal of Applied Physics*, Vol. 24, pp. 981-988.
- Lin. M. Y, Lindsay.H.M., Weitz.D.A, Ball.R.C, Klein.R and Meakin.P, Universality of fractal aggregates as probed by light scattering. *Proceedings Royal Society of London Bulletin*, A 423,71-87,1989.
- Choi, J., Tripathi, S., Hansen, D., Dornfeld, D.A. 2006, Chip scale prediction of nitride erosion in high selective STI CMP, 2006 CMP-MIC Conference, pp. 160-167.
- Smith, T. H., Fang, S. J., Boing, D. S., Shinn, G.B., Stefani, J. A., 1999, A CMP model combing density and time dependencies, 1999 CMP-MIC, pp. 97-104.
- Stein, D., Hetherington, D., Dugger, M., Stout, T., 1996, Optical interferometry for surface measurement of CMP pads, *Journal of Electronic Materials*, Vol. 25, pp. 1623-1627.
- Wang, C., Sherman, P. J., Chandra, A., 2005, A stochastic model for the effects of pad surface topography evolution on material removal rate decay in chemical-mechanical planarization, *IEEE Transactions on Semiconductor Manufacturing*, Vol. 18, no. 4, pp. 695-708.
- Johnson, N.L., Kotz, S., 1970, “Distributions in Statistics: Continuous Univariate Distributions,” Vol. 1, Wiley, New York.
- Baker, A. R., 1996, The origin of edge effect in chemical mechanical planarization, *Proceeding of Electrochemical Society Meeting*, Vol. 96, pp. 228.
- Ouma, O. 1998, Modeling of chemical mechanical polishing for dielectric planarization, Ph.D. Thesis, MIT.
- Laursen, T., Grief, M. (2002), “Characterization and optimization of copper chemical mechanical planarization,” *Journal Electronic Material*, Vol. 31, no. 10, pp. 1059–1065.



(Left) Figure 1: Global step height generated due to the different pattern density. Figure 2: Illustration of the model (Greenwood, 1966)

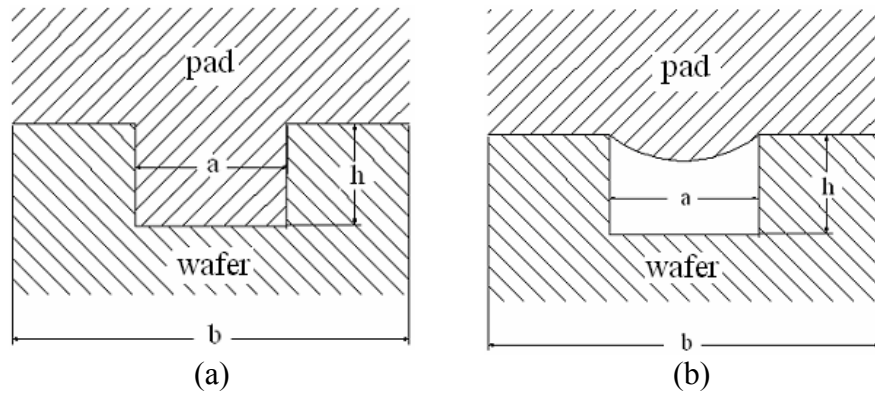


Figure 3: Schematics of the pattern wafer/pad contact interface: (a) pad contact with wafer completely (b) pad not contact with the down area of wafer.

Parameters	Values
Asperity Radius ( $R_p$ )	$50\mu\text{m}$
Standard deviation of asperity height ( $\sigma$ )	$15.625\mu\text{m}$
Skewness ( $\gamma$ )	$-1.25$
Kurtosis ( $\beta$ )	$6.875$
Asperity density ( $\eta_s$ )	$2 \times 10^8/\text{m}^2$

Table I: Parameter values for pad asperities height

Parameters	Values
Young's modulus $E$	$29\text{MPa}$
Die scale influence length $l_d$	$3\text{ mm}$
Feature scale influence length $l_f$	Pitch length
Pad bending factor $\alpha$	$0.55 \times 10^{12}\text{ N/m}^3$
Critical contact height $H$ (for L5)	$0.11, 0.068, 0.1, 0.082, 0.09\ \mu\text{m}$

Table II: Parameter values for the simulation

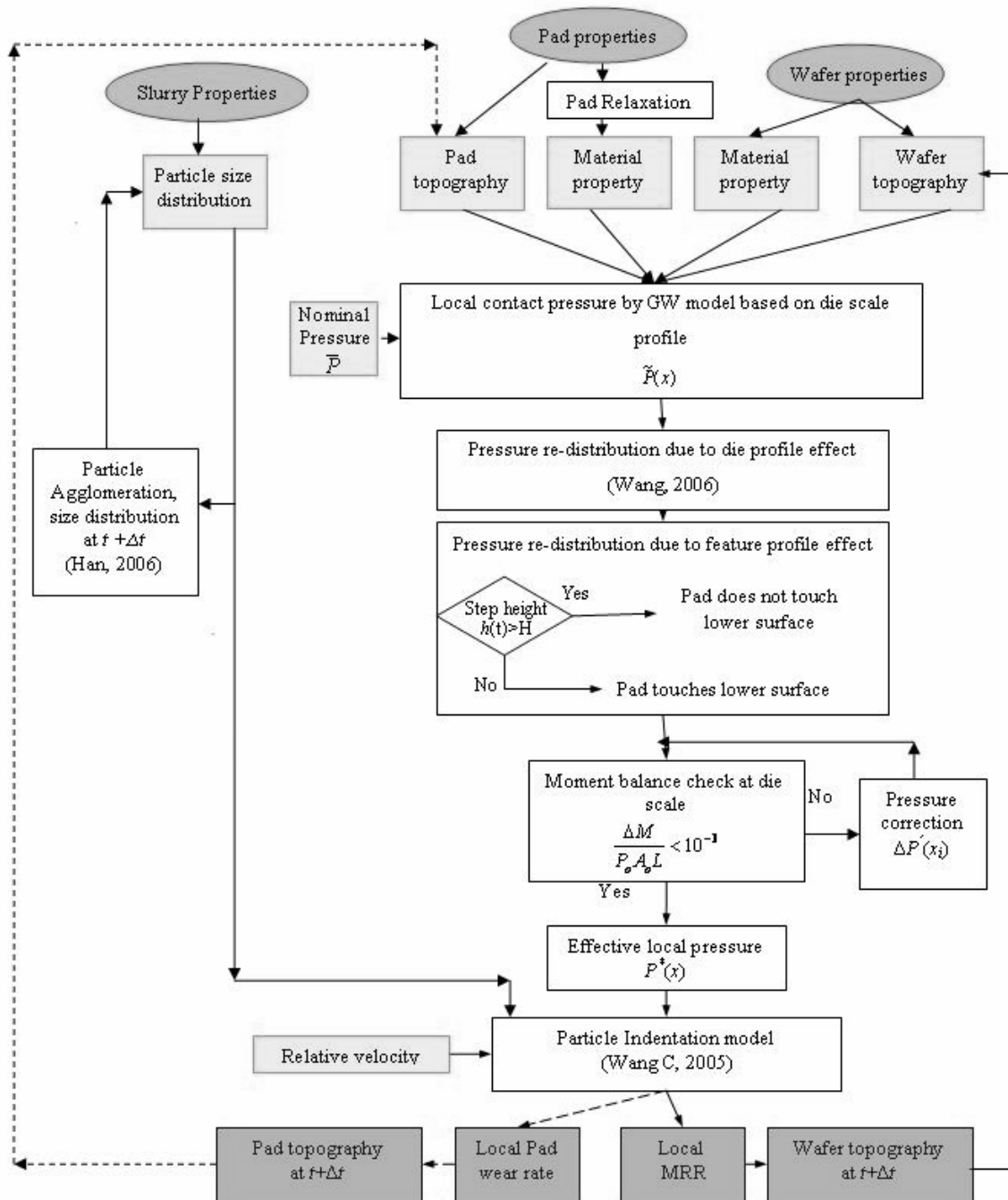


Figure 4: Simulation process flow.

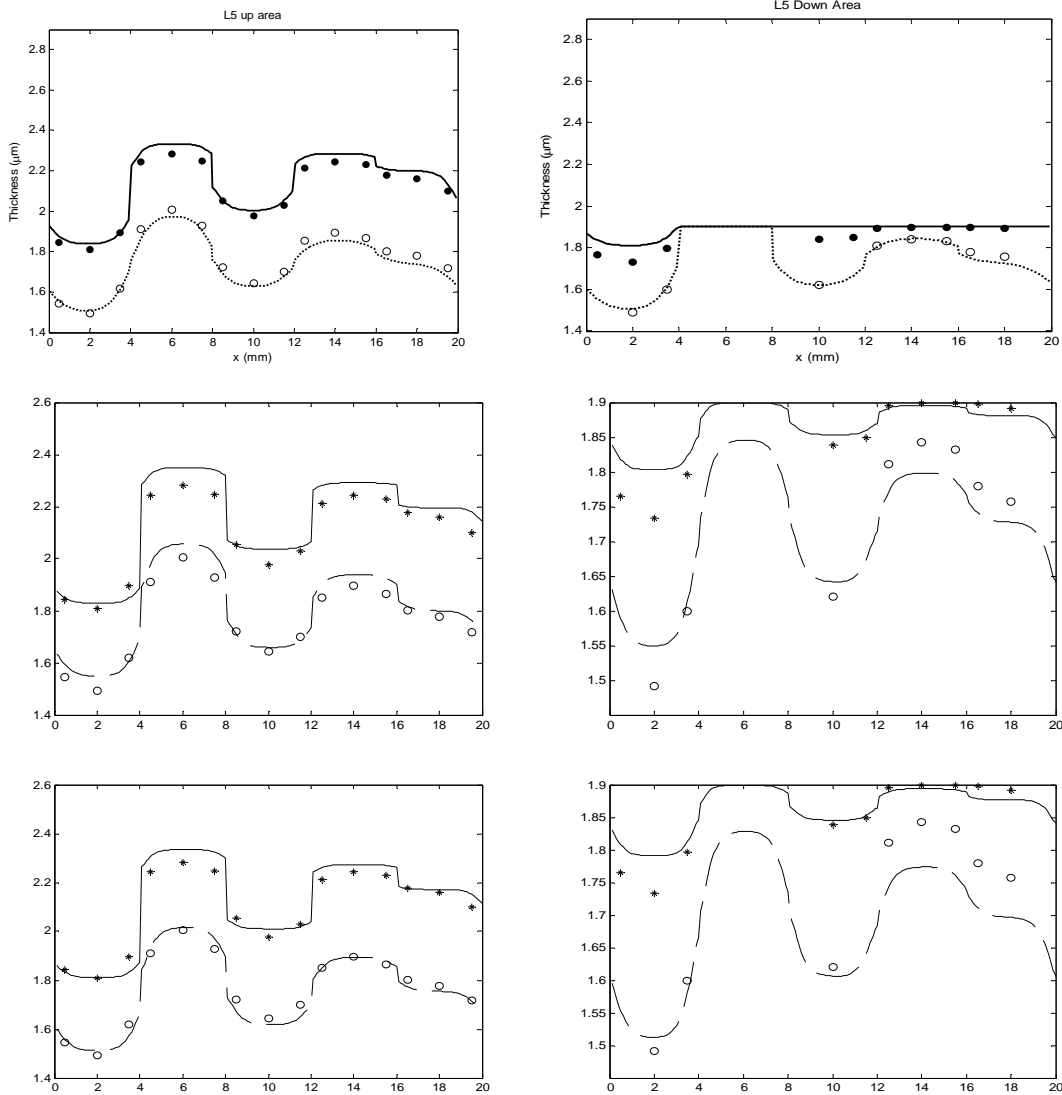


Figure 9: Comparison of predictions (lines) with experimental data(dots) (Ouma, 2002) for up area(left) and down area(right). X axis (mm) and Y axis (micron). Top: No particle or pad evolution no pad relaxation. Middle: With pad relaxation and pad, DLA particle evolution. Bottom: With pad relaxation and pad, RLA particle evolution.

Line No. on wafer	RMS Prediction Error (Å) No Agglomeration or pad evolution	RMS Prediction Error (Å) With DLA Agglomeration, Pad Evolution and Relaxation	RMS Prediction Error (Å) With RLA Agglomeration, Pad Evolution and Relaxation
L3	396	420	347
L4	418	468	379
L5	434	448	373

Table III: Prediction Error.

Time (sec)	Scratch Probability per particle – RLA Agglomeration
0	2.77E-10
20	1.21E-12
40	3.22E-13
60	1.65E-13

Table IV: Scratch Probability due to RLA Agglomeration and Pad Relaxation.